Elsevier Editorial System(tm) for Polymer
Manuscript Draft

Manuscript Number:

Title: The fundamentals of flame treatment for the surface activation of polyolefin polymers - a review

Article Type: Feature Article

Section/Category: Physical Chemistry of Polymers

Keywords: coatings; polymer science and technology; surface energy.

Corresponding Author: Dr. Stefano Farris, Ph.D.

Corresponding Author's Institution:

First Author: Stefano Farris, Ph.D.

Order of Authors: Stefano Farris, Ph.D.; Simone Pozzoli, Dr; Paolo Biagioni, Ph.D.; Lamberto Duò, Prof.; Stefano Mancinelli, Dr.; Luciano Piergiovanni, Prof.

Abstract: This paper aims to provide an exhaustive and comprehensive overview on flame treatment as a valuable technique for improving the surface properties of polymers, especially polyolefins. It starts with a brief historical excursus on the origin of flame treatment, and the second section deals with the major fundamentals of flame chemistry, with a special focus on the combustion process and mechanism of surface activation. The most important parameters influencing the extent of the oxidation reaction along with relevant practical notes are discussed in the third section. The concluding section outlines how the most significant features of flame treatment can be profitably used to improve the wettability and adhesion properties of polyolefin surfaces, especially from the perspective of developing novel composite solutions such as polyolefins/bio-based coating pairs intended for many different applications.

*Graphical Abstract

The fundamentals of flame treatment for the surface activation of polyolefin polymers

Stefano Farris,[1*] Simone Pozzoli,[1] Paolo Biagioni,[2] Lamberto Duó,[2] Stefano Mancinelli[3] and Luciano Piergiovanni[1]

[1] *DiSTAM, Department of Food Science and Microbiology, Packaging Laboratory –University of Milan, Via Celoria 2 – 20133 Milan, Italy*
[2] *LNESS, Department of Physics, Politecnico di Milano, Piazza L. da Vinci 32 – 20133 Milan, Italy*
[3] *esseCI srl Company, Via Flaminia Ternana n. 386 – 05035 Narni, Italy*

Graphical abstract

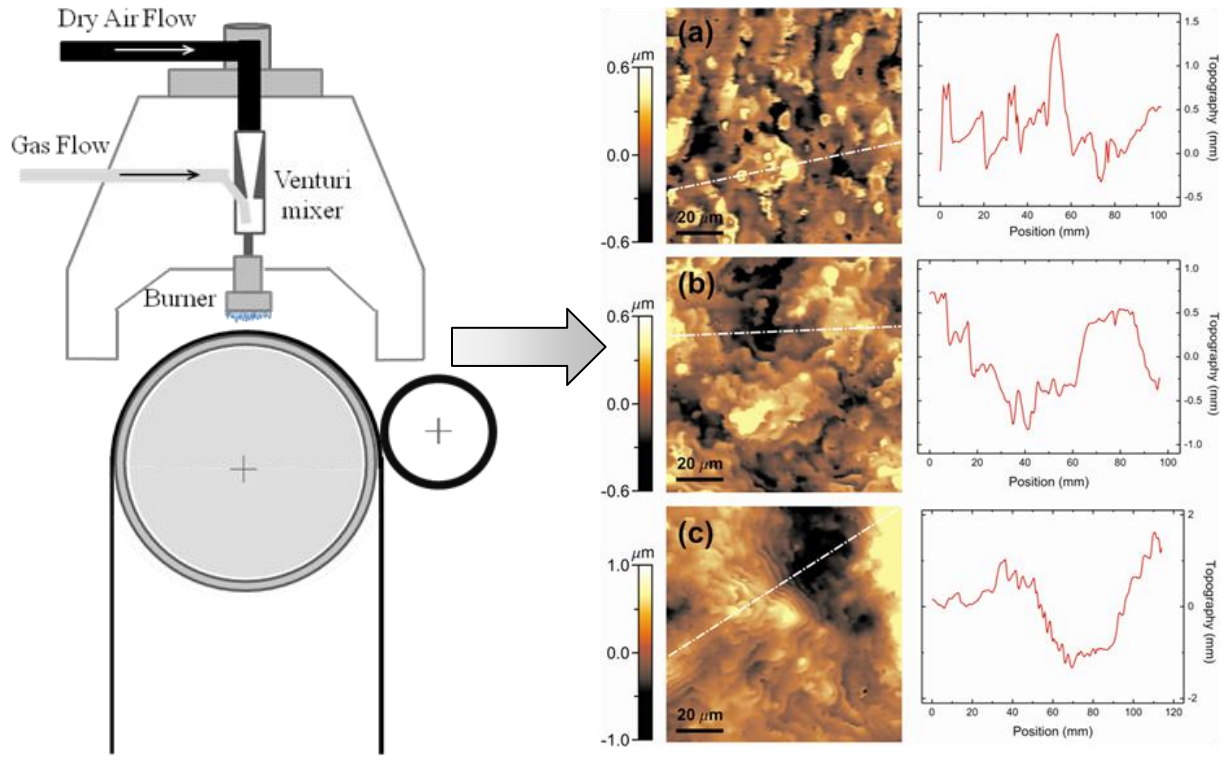

The fundamentals of flame treatment for the surface activation of polyolefin polymers – a review

Stefano Farris,[1*] Simone Pozzoli,[1] Paolo Biagioni,[2] Lamberto Duó,[2] Stefano Mancinelli,[3]

Luciano Piergiovanni[1]

[1] DiSTAM, Department of Food Science and Microbiology, Packaging Laboratory –University of Milan, Via Celoria 2 – 20133 Milan, Italy

[2] CNISM-Department of Physics, Politecnico di Milano, Piazza L. da Vinci 32 – 20133 Milan, Italy

[3] esseCI srl Company, Via Flaminia Ternana n. 386 – 05035 Narni, Italy

*Corresponding author. Tel.: +39 0250316654; fax: +39 0250316672

E-mail address: stefano.farris@unimi.it (S. Farris)

Abstract

This paper aims to provide an exhaustive and comprehensive overview on flame treatment as a valuable technique for improving the surface properties of polymers, especially polyolefins. It starts with a brief historical *excursus* on the origin of flame treatment, and the second section deals with the major fundamentals of flame chemistry, with a special focus on the combustion process and mechanism of surface activation. The most important parameters influencing the extent of the oxidation reaction along with relevant practical notes are discussed in the third section. The concluding section outlines how the most significant features of flame treatment can be profitably used to improve the wettability and adhesion properties of polyolefin surfaces, especially from the perspective of developing novel composite solutions such as polyolefins/bio-based coating pairs intended for many different applications.

Keywords: coatings, polymer science and technology, surface energy

1. Introduction

Surface properties play a pivotal role in defining the performance of materials. Among these properties, wettability and adhesion are sought after in several industrial fields such as automotive, aerospace, building, engineering, biomedical, and biomaterials [1]. For this reason, they have been extensively studied by different branches of science such as polymer chemistry, physics, and rheology. Adhesion and wettability are of critical importance for polymers intended for packaging applications, since they can greatly affect relevant and practical attributes such as the printability of a film, the strength of a laminate, and the anti-fog property of boxes, as well as the processability, convertibility, recyclability, and biodegradability of the final materials. Worldwide attention has long been focused on those applications requiring the deposition of a layer or coating (e.g., adhesives, paints, and varnishes) onto a polymeric substrate, especially when the adhesion at their interfaces is difficult to accomplish due to the inherent chemical surface differences of the two contacting polymers. As a consequence, the establishment of both interatomic and intermolecular interactions governing the adhesion phenomenon at the substrate/coating interface is totally frustrated [2]. To make these surfaces prone to printing and coating processes, different strategies have been developed including using an adhesion promoter (e.g., chlorinated polyolefin, CPO) [3], blending ethylene-propylene rubber to form thermoplastic polyolefin (TPO) [4], and exploiting physical-chemical phenomena at the base of plasma [5], corona [6], laser [7], and flame treatments [8]. Although all of them have been suggested as suitable approaches for enhancing polymer adhesion strength, which is the most effective and feasible one is still the subject of debate [9]. However, it is generally agreed that flame treatment, together with corona discharge, is the most widely used for the surface activation of polyolefin substrates [10].

The development of flame treatment has proceeded hand in hand with that of polyolefins [11]. After the early pioneer work of W.H. Kreidl, a considerable drive towards industrial implementation arose after the discovery of isotactic polypropylene (PP) by Giulio Natta in 1954. At that time, researchers belonging to the Montecatini Company located in the chemical district of

Terni started working on Moplen® in an attempt to find a solution to the high recalcitrance of such a polymer to printing and coating [12]. In those same years, the electrical corona discharge process was being set up by Kreidl's assistant, Kritchever, with the same goal of improving the surface properties of polyolefins. Thereafter, the use of such a process grew tremendously and has become the primary method of treating polymer films for two main reasons: firstly, because of concerns about the safety of open flames in industrial environments and secondly, as a consequence of the recognised sensitivity of flame treatments to small changes in process conditions [13]. As a result, although originally developed to treat films, up to the beginning of the new century flame treatment has chiefly been used for cellulosic (paper and paperboard) or relatively thick polyolefin materials (e.g., automobile body parts and blow-moulded bottles) under the common misconception that corona treatment is more suitable for polyolefinic films, whereas flame treatment is preferred for tridimensional symmetrical shapes.

Over the past two decades many remarkable innovations, which will be discussed later in this review, have contributed to the renewed interest in flame treatment, making it a recognised technique for modifying film surfaces as well as tridimensional objects. However, to fully exploit the potential of this technique, it seems of primary importance to acquire a deep knowledge of the overall process. For this purpose, this review has been conceived as firstly a collection of the most relevant basic principles and key concepts of flame treatment, with special emphasis on the fundamental chemistry governing both the flame and surface activation phenomena. Secondly, this paper aims to illustrate the main practical parameters to make the process successful. The conclusion is dedicated to a brief discussion on the future trends in this field, illustrating how flame treatment can help in the design of new high performance packaging materials.

2. Flame chemistry

In 1848, Michael Faraday inaugurated the 'Christmas Lectures' at the English Royal Institute with a talk entitled "The chemical history of a candle", starting with the following words: "There is no better, there is no more open door by which you can enter into the study of natural philosophy than by considering the physical phenomena of a candle" [14]. Approximately 150 years later, worldwide scientists can only agree with this leading opinion, since an apparently trivial process indeed governs many modern human activities. In addition, such a process paved the way for theoretical research topics that, in most cases, found remarkable applications in many fields. One example is the treatment of plastic objects in a flame, which makes them suitable adherends. Combustion is a complex process involving many chemical reactions between a fuel (generally a hydrocarbon) and an oxidant (e.g., the oxygen in the air) with the production of heat and (although not always) light in the form of a flame. Migration of chemical species within the flame results in a subsonic wave (40–45 cm s^{-1} in air/hydrocarbon systems) supported by combustion [15]. Although a huge variety of chemical reactions take place during combustion, leading to many active radical species, it is generally recognised that the overall process can be summarised in few main steps, as schematically displayed in Figure 1.

2.1. Initiation

This first step is represented by the general following reaction, where M is the reactant molecule, $R^{\cdot}$ the radical species and K_1 the reaction rate:

$$M \xrightarrow{k_1} R^{\cdot} \quad (1)$$

Firstly, the lowest-energy configuration of the dioxygen molecule (O_2), which is a stable, relatively unreactive diradical in a triplet spin state, is forced into a spin-paired state, or singlet oxygen ($^1O_2$). This is normally achieved by the absorption of sufficient energy supplied as heat (ignition).

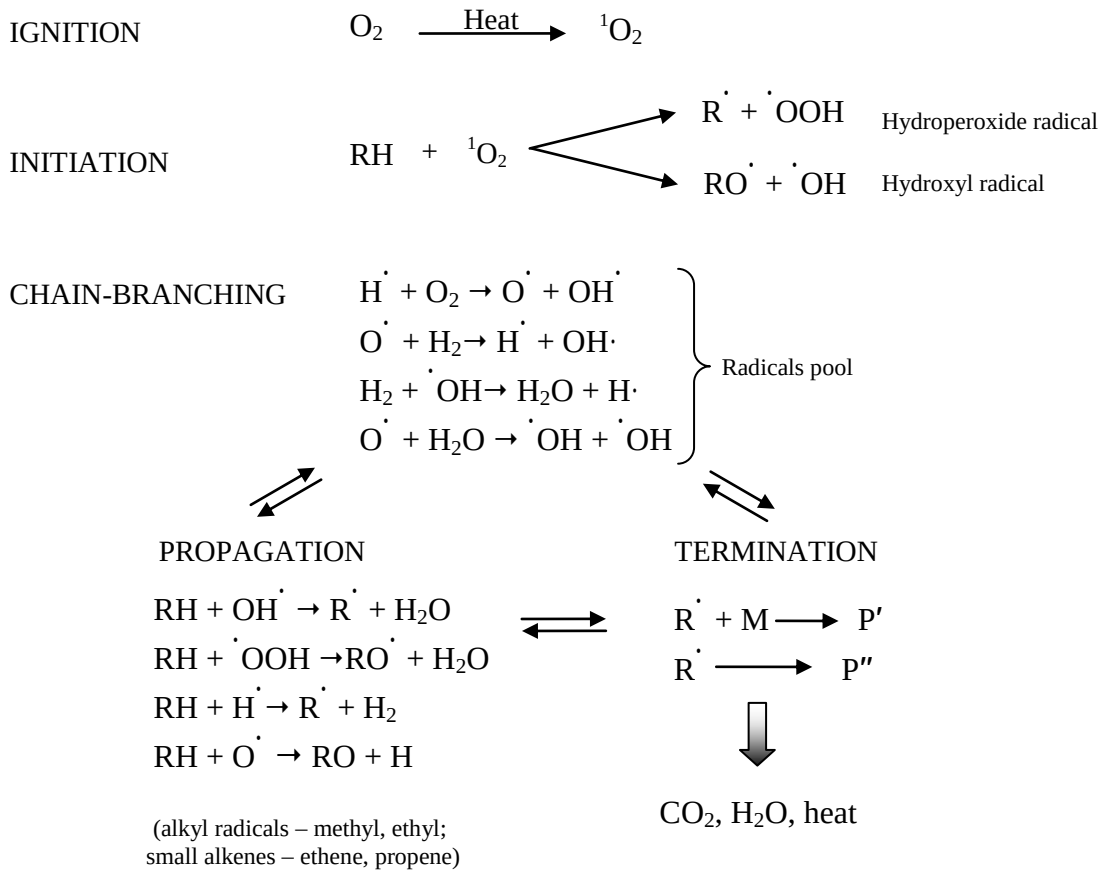

Figure 1. Schematic overview of the combustion process.

The diradical form of oxygen is in a triplet ground state because the electrons have parallel spins. If triplet oxygen absorbs sufficient energy to reverse the spin of one of its unpaired electrons, it will form the singlet state, in which the two electrons have opposite spins. This activation overcomes the spin restriction, and singlet oxygen can consequently participate in reactions involving the simultaneous transfer of two electrons (divalent reduction). Since paired electrons are common in organic molecules, singlet oxygen is much more reactive towards organic molecules than its triplet counterpart. At this point, the so-called hydrogen abstraction from the fuel to oxygen can take place and hydroperoxide ($^{\cdot}$OOH) and hydroxyl ($^{\cdot}$OH) radicals are formed:

$$RH + {}^1O_2 \rightarrow R^{\cdot} + {}^{\cdot}OOH \quad (1a)$$

$$RH + {}^1O_2 \rightarrow RO^{\cdot} + {}^{\cdot}OH \quad (1b)$$

2.2. Chain branching

This step can be schematically represented by the following mechanism, where M and M′ are the reactant molecules, $R^{\cdot}$ the radical species, α a multiplicator factor and K_2 the reaction rate:

$$R^{\cdot} + M \xrightarrow{k_2} \beta R^{\cdot} + M' \quad (2)$$

Many different radical species (radical pool) are formed primarily by a general oxyhydrogenation reaction pattern:

$$H^{\cdot} + O_2 \rightarrow O^{\cdot} + OH^{\cdot} \quad (2a)$$

$$O^{\cdot} + H_2 \rightarrow H^{\cdot} + OH^{\cdot} \quad (2b)$$

$$H_2 + {}^{\cdot}OH \rightarrow H_2O + H^{\cdot} \quad (2c)$$

$$O^{\cdot} + H_2O \rightarrow {}^{\cdot}OH + {}^{\cdot}OH \quad (2d)$$

Among them, Reaction (2a), which is promoted by H radicals arising from the dissociation of hydrogen at temperatures above 400°C, seems to be the most important since it generates all the successive reactions [(2b)–(2d)]. It has to be pointed out that, since the rate of Reaction (2a) is smaller than the rate of the reaction between a hydrocarbon and the hydrogen radical, the presence of the hydrocarbon actually inhibits the formation of the radical pool [13].

2.3. Propagating step forming product

The highly reactive free radicals formed can freely interact with the hydrocarbon through the previously mentioned hydrogen/abstraction mechanism and according to the following general mechanism, where M is the reactant molecule, $R^{\cdot}$ the radical species, P the new formed product, and K_3 the reaction rate:

$$R^{\cdot} + M \xrightarrow{k_3} R^{\cdot} + P \quad (3)$$

The final result is the formation of new products as well as additional radical species:

$$RH + OH^{\cdot} \rightarrow R^{\cdot} + H_2O \quad (3a)$$

$$RH + {}^{\cdot}OOH \rightarrow RO^{\cdot} + H_2O \quad (3b)$$

$$RH + H^{\cdot} \rightarrow R^{\cdot} + H_2 \quad (3c)$$

$$RH + O^{\cdot} \rightarrow RO + H \quad (3d)$$

Hydrogen, methyl, and ethyl radicals and small alkenes (primarily ethene) can be produced from the fuel degradation occurring during hydrogen abstraction. Subsequent thermal decomposition can give rise to smaller alkyl radicals, small alkenes, and alkynes (acetylene) by thermal decomposition [13].

2.4. Termination step forming product

The termination phase is basically made of two distinct processes:

$$R^{\cdot} + M \xrightarrow{k_4} P' \quad (4)$$

$$R^{\cdot} \xrightarrow{k_5} P'' \quad (5)$$

In step (4), radicals ($R^{\cdot}$) react with other molecules (M) at a specific rate (K_4) to give new unreactive species (P'), whereas in step (5) the radicals themselves ($R^{\cdot}$) evolve to new unreactive species (P'') at a defined rate (K_5).

The two main reactions involved in this final step are, respectively, CO formation and its oxidation to CO_2. CO formation takes place starting from all those small molecules originating from the previous step. In particular, methyl and ethyl radicals and small alkenes (e.g., ethene) are the most important intermediates leading to the formation of carbon monoxide through an oxidative attack. The oxidation of CO to CO_2 is the concluding step of hydrocarbon combustion, according to the main reaction:

$$CO + OH^{\cdot} \rightarrow CO_2 + H^{\cdot} \quad (6)$$

Together with the reaction represented by Eq. (2a), the above mechanism (Eq. 6) plays a dominant role within the combustion of hydrocarbons [16]. The main route to the carbon dioxide is the oxidation of carbon monoxide by OH radicals, whereas the contribution by O atoms is considered negligible [16]. Analogously to the rate of the reaction between the H radical and oxygen in a

157 typical oxyhydrogenation scheme (Eq. 2a), OH radicals react more rapidly with hydrocarbons than
158 with CO to form CO_2. As a consequence, it can be asserted that hydrocarbons actually inhibit the
159 formation of CO_2. In other words, the rate of the oxidation of CO climbs considerably as soon as
160 both the original fuel and all hydrocarbon intermediates have been consumed, since the hydroxyl
161 radical concentration rises dramatically [13].
162 In these final steps, other reactions take place, among which it is worth mentioning the water
163 formation by different pathways. Water forms through the reaction:

164 $$RH_x + OH^{\cdot} \rightarrow RH_{x-1} + H_2O \quad (7)$$

165 by the oxidation of formaldehyde (an intermediate of the combustion process):

166 $$CH_2O + OH^{\cdot} \rightarrow CHO^{\cdot} + H_2O \quad (8)$$

167 starting from hydrogen radicals formed by previous reactions:

168 $$H^{\cdot} + OH^{\cdot} + M \rightarrow H_2O + M \quad (9)$$

169 and through a typical oxyhydrogenation pattern (e.g., Eq. 2c).

170 ## 3. Explosive behaviour and the 'runaway reaction'

171 It is worth noting that, considering the sequence [(2)–(5)], when:

172 $$\beta > \beta_{crit.} = 1 + \frac{k_4 + k_5}{k_2}, \quad (10)$$

173 the combustion system has reached the explosion condition. This means that if the air/hydrocarbon
174 mix is within its flammability limits (i.e., it has a suitable composition) and within its explosive
175 conditions (i.e., within adequate pressure/temperature boundaries for the same composition), the
176 flame is generated and can spontaneously propagate. Of course, according to Equation (10), the
177 higher the rate of the chain branching step (K_2) and the lower the rates of the termination steps (K_4
178 and K_5), the higher the probability for the explosion of the combustion system to occur. When so,
179 Reactions (2a)–(2d) continuously increase the number of reactive radicals, allowing the exothermic

condition to be approached by the combustion system. Since the rate of the above-reported reactions (and thereby the rate of the heat released) increases exponentially with temperature (according to the Arrhenius law), the fuel/oxidant mixture becomes explosive. Therefore, Reactions (2a)–(2d) are greatly important in the oxidation reaction mechanism of any hydrocarbon because they allow the propagation of the flame. This exothermic reaction is also called the 'runaway reaction', which occurs when the reaction rate increases because of an increase in temperature, causing a further increase in temperature and a further increase in the reaction rate. Since direct combustion by atmospheric oxygen in a flame is a reaction mediated by radical intermediates, the conditions for radical production are guaranteed by thermal runaway, where the heat generated by combustion is necessary to maintain the high temperature for radical production. The 'runaway reaction' is, therefore, the key condition for radical production.

4. Laminar flame profile

A laminar flame (which is ordinarily employed by flame treaters) is defined as a mixture of a fuel and an oxidiser, thoroughly premixed before combustion. The term 'premixed laminar flame' is interchangeable with the term 'deflagration' to indicate the propagation of the combustion process accompanied by a decrease in both density and pressure together with an increase in velocity (contrary to the propagation known as 'detonation'). Within a laminar flame profile, three main zones can be observed (Figure 2), which correspond to specific reactions. As a consequence, different thermal gradients and reactive species can be encountered. These zones are briefly described here.

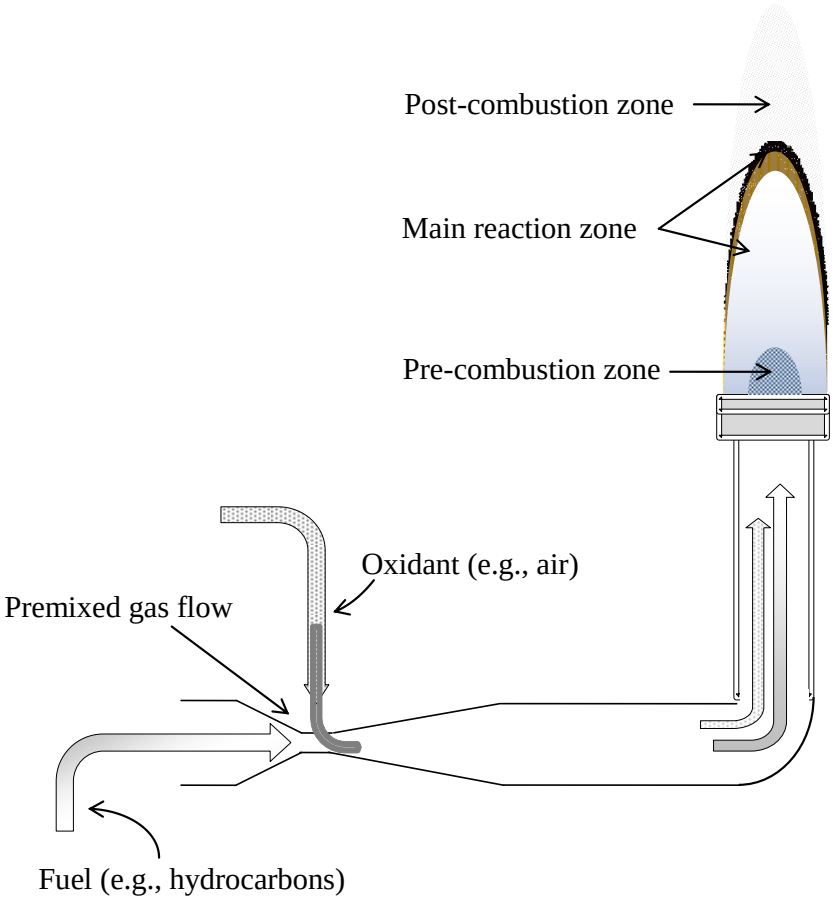

Figure 2. Main zones in a laminar flame profile.

1) *Pre-reaction zone*

This region, also called the 'dark zone', has a typical dark bluish colour. It is the coldest region of a flame because even though some of the hydrogen formed is oxidised to water the combustion process has not yet reached the explosion condition, and thereby the amount of net energy released is negligible. In this region, the only abundant free radical is the hydrogen atom, which reacts quickly with hydrocarbons and oxygen, thereby impeding the formation of the radical pool. For this reason, this zone is also known as the 'reducing zone'. This is an ineffective and unimportant region for surface activation purposes, since it in no way contributes to the oxidation of the plastic substrate.

2) *Main reaction zone*

Also called the 'luminous zone', the mixed reaction zone is characterised by the highest temperature of the combustion system (for propane-based mixtures the temperature reaches 1900–2000°C). In this zone, radical content increases dramatically to the detriment of the reactant concentration. The high concentration of radical species makes this region strongly oxidising, in contrast to the reducing zone mentioned above. Such an oxidising region is valuable for making effective the flame treatment of polyolefins. The colour of this zone depends on the fuel/air ratio: a deep bluish violet radiation, with the flame becoming almost transparent if the quantity of gas is increasingly reduced, is produced when the mixture is gas-lean (due to excited CH radicals); conversely, a green radiation appears when the mixture is gas-rich (due to excited C_2 molecules). When the gas in the mixture increases still further, the radiation turns yellowish because of the carbon particles formed. The observation of the colour of the flame is an empirical tool widely used by the operators of flame treatment plants to keep the right mixture composition throughout the process.

3) *Post-combustion zone*

This is the largest of the three regions found in a typical laminar flame profile. The temperature here remains high due to the exothermic oxidation reaction (partial or complete) of CO into CO_2, with a release of heat. Although intermediate species such as CH_3, C_2H_2, and CH_2O are typical of the luminous region only, radicals such as $H^{\cdot}$, $OH^{\cdot}$, and $O^{\cdot}$ can also be detected in the post-combustion zone [17]. Generally speaking, the concentration of radicals in a laminar flame profile accounts for approximately 10^{-3} relative to the reactants, whereas ion species (among which the H_3O^+ is the most abundant) are decidedly less (10^{-6} relative to the reactants). Normally, they lie slightly beyond the luminous portion of the flame [13].

The existence of a profile of compositional differences over a laminar flame can be explained in terms of the convective flows of unburned gases from the dark zone to the luminous zone and the

238 diffusion of radical species from the high temperature zone to the pre-heating region, in the opposite
239 direction to the convective flow. In particular, the diffusion of radical species is dominated by
240 hydrogen atoms, which do not participate to the chain branching step described by Equation (2a)
241 because of the lower temperature in the dark region. Instead, H atoms combine with oxygen radicals
242 in the pre-heating zone to yield a large amount of $HOO^{\cdot}$ radicals. These then form hydrogen
243 peroxide (H_2O_2), which does not dissociate because of the low temperatures in the dark zone. H_2O_2
244 is then conveyed to the luminous zone by convective flows, where the temperature conditions make
245 possible the formation of $OH^{\cdot}$ radicals. This explains the high concentration of OH radicals relative
246 to $O^{\cdot}$ and $H^{\cdot}$ in the early part of the luminous zone and the very high temperature reached there,
247 with the OH radicals-forming reaction highly exothermic (~85 kcal mol^{-1}). In addition, it explains
248 why the $OH^{\cdot}$ attack on the fuel is the primary route for fuel degradation.

249 Finally, it is worth noting that combustion processes are never complete. In the combustion of
250 hydrocarbons, both unburned carbon and carbon compounds (such as CO and others) are always
251 present. In addition, when air is the oxidant, like in a typical flame treater plant, some nitrogen can
252 be oxidised to various nitrogen oxides (NO_x) [18]. For example, Pijpers and co-workers observed a
253 significant amount of N at the surface of PP samples at air/propane ratios between 26 and 18 [8].
254 Although different mechanisms can lead to the formation of NO_x compounds, in commonly used
255 burners the high temperature oxidation of molecular N_2 seems to be the preferred way to form NO_x,
256 among which nitrogen monoxide (NO) is the most abundant. The term 'thermal NO' is widely
257 accepted to indicate the formation of NO from the N_2 present in the combustion air. This process
258 requires very high temperatures (~1500°C) to break the covalent triple bond in the N_2 molecule by
259 the attack of the O radical produced during the combustion process. The formation of NO is in an
260 inverse proportion to CH_x intermediates and CO emissions when varying the air/fuel ratio. In
261 particular, NO formation is promoted by increased temperatures, residence times, and O_2

concentrations. Therefore, controlling NO formation during treatment operations can be easily achieved by burning under lean conditions and flame quenching using a secondary air stream. Besides NO, nitrogen dioxide (NO_2) is a minor product of the combustion process [19]. However, since the NO oxidises to NO_2 in the atmosphere NO is a potential precursor of NO_2.

5. Laminar flame speed and stability

As previously stated, in a combustion system the flame is a subsonic wave characterised by a velocity called laminar flame speed, which is defined as the velocity at which unburned gases move throughout the combustion wave in the direction normal to the wave surface [20]. Different theories have been developed over time to provide an insightful description and quantification of flame speed. Some of them (e.g., the Tanford–Pease theory [21]) are based on the diffusion of the huge variety of chemical species produced during combustion throughout the front of the flame. Accordingly, such diffusion depends on the species' molecular weights, meaning that low mass species (H, H_2, O, and OH) will diffuse more rapidly than the heavier ones. In particular, besides its dominant role in Reaction (2a), hydrogen atom diffusion is especially important since its high diffusion rate is responsible for the main phenomena connected with laminar flames [16]. Other theories, generally called 'thermic', are instead based on the diffusion of heat rather than chemical entities. Among them, the theories of Zeldovich–Frank-Kamenetskii [22], Semenov [23,24], and Mallard–Le Chatelier [25] deserve to be mentioned because they similarly contribute to the chemical kinetic modelling of hydrocarbon combustion.

A generalisation arising from the combination of these theories has been suggested as the most appropriate approach to model laminar burning velocity, since it makes possible fixing the most important practical parameters in laminar flame propagation, which are otherwise difficult to interpret in more complex analyses [20]. Accordingly, it is assumed that there are two main mechanisms governing flame propagation – the convection of heat and the diffusion of chemical species – in a back-and-forward modality, namely from the combustion zone to the zone of

unburned gas and vice versa. Thus, the flame can be seen as an array of adjacent waves formed by unburned gas at always higher temperatures until the ignition of the gas is reached. For the assumption that the premixed combustion is one-dimensional and steady (contrary to turbulent, non-premixed flames), the temperature profile along a flame can be schematically split into three different regions, as qualitatively depicted in Figure 3, where the enthalpy of formation diagram is also reported.

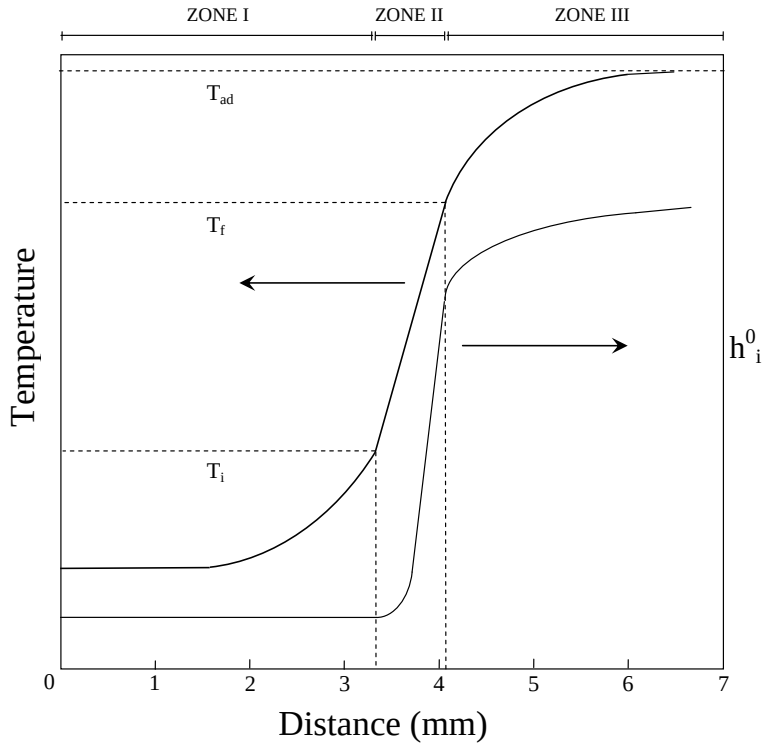

Figure 3. Spatial evolution of temperature and enthalpy of formation in a premixed laminar flame.

In the first zone, the initial temperature (T_0) rises exponentially, whereas the enthalpy of formation (h_i^0) remains at the same values of the starting mix. This means that in this first region the combustion conditions have not yet been reached. Heat-releasing reactions of low entities can anyhow occur, such as oxygen attacks on the hydrocarbon, hydrogen abstraction onto the hydrocarbon backbone (due to radicals diffusing from the main reaction zone), and scission/condensation reactions of the fuel. In this first zone, therefore, the temperature is controlled

by both diffusion and convection. The boundary between zone I and zone II is the point where the ignition takes place. At this point, the temperature registered is called the 'mixture ignition temperature' (T_i). In the second zone, temperature and enthalpy behave similarly, i.e., both increase linearly within a very narrow spatial range. It is assumed that in this zone the convection and generation of new species are the most important reactions, with the diffusion contribution negligible. The boundary between zone I and zone II is called the 'flame temperature' (T_f), i.e., the temperature of burning. Finally, in the third region both the temperature and enthalpy increase slowly because of the almost total absence of radicals. In this last step, carbon monoxide is oxidised to carbon dioxide and radical species combine into more stable molecules. Finally, the system reaches the so-called adiabatic temperature (T_{ad}), i.e., the temperature at which the heat release to the surroundings stops.

The theoretical treatment for the computation of the flame speed starts with the assumption that within zone I the heat coming from zone II by convection equals the heat required to raise the temperature of the unburned gases to the ignition temperature (T_i). Secondly, it is assumed that the increase in temperature between adjacent gas layers is constant. In other words, this means that the slope of the temperature curve is linear, and thereby can be approximated by the expression $[(T_f–T_i)/\delta]$, where δ is the thickness of the reaction zone. From the enthalpy balance the following equation can be obtained:

$$mc_p = \lambda \frac{(T_f - T_i)}{\delta} A \qquad (11)$$

where λ is the thermal conductivity, m is the mass rate of the unburned gas mixture into the combustion wave, and A is the cross-sectional area assumed as unity [20]. According to the one-dimensional feature of the problem, the mass rate m can be expressed as:

$$m = \rho A u = \rho A S_L \,, \qquad (12)$$

where ρ is the unburned gas density, u is the velocity of the unburned gases, and S_L is the symbol for laminar flame velocity. As unburned gases enter normal to the wave, by definition it can be written $S_L = u$. Therefore, Equation (11) becomes:

$$\rho S_L c_p (T_i - T_0) = \lambda (T_f - T_i)/\delta \tag{13}$$

Thus. the equation for the computation of the flame speed can be easily inferred:

$$S_L = \frac{\lambda}{\rho c_p}\left(\frac{T_f - T_i}{T_i - T_0}\right)\frac{1}{\delta} \tag{14}$$

where c_p is the specific heat capacity of the fuel. From Equation (14) it is possible to observe the direct relationship between flame speed (S_L) and flame temperature (T_f), i.e., the higher the flame speed, the higher the flame temperature. It allows us to talk about flame temperature and flame speed interchangeably. Unfortunately, in the above equation, the term δ (the reaction zone thickness) is unknown; nevertheless, it can be related to flame speed by the following expression:

$$\rho u = \rho S_L = \omega \delta, \tag{15}$$

which assumes the total mass per unit area entering the reaction zone is equal to the mass consumed in that zone for the steady flow problem being considered. In Equation (15), ω is the reaction rate in terms of concentration (grams per cubic cm) per unit time. Equation (14) can, therefore, be rewritten as:

$$S_L = \left[\frac{\lambda}{\rho c_p}\left(\frac{T_f - T_i}{T_i - T_0}\right)\frac{\omega}{\rho}\right]^{1/2} \sim \left(\alpha \frac{\omega}{\rho}\right)^{1/2} \tag{16}$$

where ρ is the unburned gas density and α is the thermal diffusivity. More specifically:

$$\alpha\ (m^2 s^{-1}) = \frac{\lambda}{\rho c_p}\frac{(W\, m^{-1}\, K^{-1})}{(kg\, m^{-3})(J\, kg^{-1}\, K^{-1})} \tag{17}$$

The denominator in Equation (17) is known as the volumetric heat capacity (J m^{-3} K^{-1}). Thermal diffusivity can ultimately be defined as the ratio of thermal conductivity to volumetric heat

capacity. In practice, thermal diffusivity is a measure of the ability of a given substance (or a mixture, as in the case of a flame) to rapidly adjust its temperature to that of the surroundings. Since the mass of reacting fuel mixture consumed by the laminar flame is given by:

$$\rho S_L \sim \left(\frac{\lambda}{c_p}\omega\right)^{1/2} \tag{18}$$

combining Equations (15) and (18) yields the following expression:

$$\delta \sim \frac{\alpha}{S_L} \tag{19}$$

From Equation (19) the average thickness of the luminous zone for a laminar flame can easily be drawn. Since, for hydrocarbon flames, the value of α (at a mean temperature of 1300 K) and S_L can realistically be approximated to 5 cm^2 s^{-1} and 35–40 cm s^{-1}, respectively, δ assumes values close to 1.0–1.5 mm. As will be discussed later, this aspect has a valuable practical consequence to fully exploiting the benefit of a flame treatment during the surface activation of polyolefin substrates. Equation (19) also highlights the inverse proportion between the thickness of the luminous zone and flame speed. Thus, flame speed (i.e., flame temperature) should always be adjusted to a certain value of δ to treat the samples in a feasible fashion. This can also be achieved by setting the value of thermal diffusivity α, since increasing thermal diffusivity leads to an increase in flame speed, as inferred from Equation (16). Therefore, for high values of α the quality of the combustion system will be enhanced due to an increase in flame temperature, which corresponds to an increase in flame treatment yield. An adequate value of α can be achieved by reducing the volumetric heat capacity of the mixture (i.e., the denominator of Equation 17), which can be obtained by decreasing the specific heat capacity of the fuel (c_p). To do so, common practice is to replace nitrogen in the fuel mixture with other lower c_p diluents such as argon or helium. It has been reported that when helium is added to a stoichiometric methane/air mixture, the flame speed is roughly threefold higher than using nitrogen (~125 cm s^{-1} vs. ~40 cm s^{-1}) [26–28].

Another aspect that should be pointed out is the effect of pressure on the flame speed of a stoichiometric air/gas mixture. The pressure dependence of flame speed is described by the following equation [20]:

$$S_L \sim \left(p^{(n-2)}\right)^{1/2} \quad (20)$$

where *n* is the overall order of the reaction. Therefore, for a given second order reaction, flame speed seems to be independent of pressure. However, by contrast, hydrocarbon/air reactions are rarely second order. Indeed, experimental data collected by several investigators suggest that the order of a general combustion process mostly falls around 1.75 [29]. This is why a reduction in flame speed is encountered with increasing pressure. A deeper comprehension of this phenomenon can be achieved by looking at the most important oxyhydrogenation reaction governing the formation of the radical pool, i.e.:

$$H^{\cdot} + O_2 \rightarrow O^{\cdot} + OH^{\cdot} \quad (2a)$$

Any reaction that inhibits the formation of H atoms or competes with the above mechanism will hinder the oxidation process, and thereby the combustion rate. For instance, the reaction:

$$H^{\cdot} + O_2 + M \rightarrow {}^{\cdot}OOH + M \quad (21)$$

clearly competes with Reaction (2a). Moreover, since it is a third order reaction, it is much more pressure-dependent than Reaction (2a). The ultimate relevant consequence is that when increasing pressure, Reaction (21) tends to slow down the overall combustion process and, thus, flame speed. Results from analytical calculations of flame speeds under different temperature/pressure conditions with detailed kinetic aspects can be found in the literature [30–33]. Moreover, it has to be mentioned that the decrease in S_L with increasing pressure becomes more pronounced for pressures above atmospheric conditions (1–5 atm). This is because, contrary to what happens at high pressures, below 1 atm Reaction (21) does not compete with Reaction (2a), and any decrease owing

392 to Reaction (21) is balanced by a rise in temperature due to chain branching step reactions such as
393 (2a).

394 At the end of this section, a final remark deserves to be stressed as far as laminar flame
395 propagation is concerned. It is nowadays accepted that although diffusion phenomena dominate in
396 initially unmixed fuel/oxidiser systems, reaction rate mechanisms prevail in premixed homogeneous
397 mixtures. It is worth emphasising that flame propagation is mostly because of the diffusion of heat
398 and mass, i.e., it is made possible by a diffusion mechanism predominantly. The role of the reaction
399 rate is instead intimately related to the thermal profile of the laminar flame, since it governs the
400 thickness of the reaction zone and temperature gradient. In other words, although the strong effect
401 of the temperature is undisputable, flame propagation has to be primarily attributed to the diffusion
402 of heat and mass. It is definitively expressed by the following expression:

403 $$S_L \sim (\alpha RR)^{1/2} \quad (22)$$

404 This states that the propagation rate is proportional to the square root of the diffusivity and the
405 reaction rate [20].

406 ## 6. Flame treatment of polyolefins

407 The term polyolefin encompasses all those polymers produced by an olefin as a starting
408 monomer, whose general formula is C_nH_{2n}. Most common polyolefins in the packaging field are
409 polyethylene (PE) and PP. Although they have different specific properties, it is recognised that
410 both polymers are inherently hydrophobic, which is in turn responsible for their typical poor
411 wettability, especially to waterborne systems. For this reason, polyolefins generally need to be
412 surface-activated before the deposition of inks, paints, adhesives, metals, and coatings. Flame
413 treatment is a valuable technique to improve the surface energy of polyolefins, although it has been
414 exploited to a minor extent with respect to corona treatment so far. However, because of
415 improvements in safety conditions as well as in some technical aspects, it is receiving renewed

attention, especially by those sectors (e.g., packaging) that historically lagged behind in the exploitation of the technique.

It has been reported that the surface activation of polyolefins by flame treatment is based on the free radical degradation mechanism, which occurs at the tertiary carbon of the PP chain and according to a random attack in the case of PE [34]. Two main steps are involved in the oxidation process of PP: 1) the breakage of the C-H links along the polymer surface by the high temperature generated by the combustion process (~1700–1900°C); and 2) the insertion of oxygen-based groups corresponding with the broken links, leading to newly available hydrophilic sites for the interaction between coating and substrate. In particular, the oxidation of methyl groups ($–CH_3$) into $–CH_2OH$ groups following treatment has been judged the most relevant surface chemistry change affecting both the wettability and adhesion properties of polyolefin substrates [35]. The generally accepted scheme is reported below:

$$RH \rightarrow R^{\cdot} + H \quad (23)$$

$$R^{\cdot} + O_2 \rightarrow ROO^{\cdot} \rightarrow ROOH \rightarrow \text{oxidised products} \quad (24)$$

It seems that the oxidation process is principally mediated by the $OH^{\cdot}$ radicals in the flame. To elucidate the chemical changes onto the polyolefins' surface following flame treatment, several techniques have been used. In particular, X-ray photoelectron spectroscopy, also called ESCA (electron spectroscopy for chemical analysis), and static secondary ion mass spectroscopy (SSIMS) have confirmed an increased level of oxidation, as demonstrated by new functionalities formed on the polyolefins' surface, such as hydroxyl, carbonyl, and carboxyl groups [36–38]. However, it has been ascertained that, working conditions being equal, more oxygen is incorporated onto PE films than PP films after flame treatment. In addition, it has been proven that the majority of the oxygen added to PP by the flame is in the form of hydroxyl species, which account for approximately 20–30% [39]. Nitrogen fixation has also been detected as a consequence of treatment, although it seems to occur on PE samples rather than PP. Nevertheless, the fixation of nitrogen is quantitatively less

important than oxygen fixation, as revealed by ESCA measurements (N/C atomic ratios < 0.03; O/C atomic ratios > 0.1–0.2) [40]. The mechanism responsible for the modification of the PP surface caused by the hydrocarbon flame has been brilliantly elucidated by Strobel and co-workers [13]. Arising from their work, it seems that the polymer radical formation occurs primarily by hydrogen abstraction because of the free radicals in the flame, such as O atoms, H atoms, and OH radicals, according to the following reactions:

$$RH + O \rightarrow R^{\cdot} + OH \quad (25)$$

$$RH + OH \rightarrow R^{\cdot} + H_2O \quad (3a)$$

$$RH + H \rightarrow R^{\cdot} + H_2 \quad (3c)$$

where $R^{\cdot}$ is a an alkyl radical. Not only can the radical species in the flame provoke polymer radical formation, but so can the thermal effect according to the mechanism:

$$RH \rightarrow R^{\cdot} + H \quad (26)$$

Based on the results obtained using a combustion mode [41], and considering that the reactivity of the H atom for hydrogen abstraction is three to five orders of magnitude inferior than the reactivity of O and OH [42], the authors concluded that, at a specific equivalence ratio of 0.93, OH radicals, O atoms, and heat are the driving forces for polymer radical formation. Most alkyl radicals formed during the previous steps (Eqs. 25–26) react with oxygen atoms, generating polymer alkoxy radicals [43]:

$$R^{\cdot} + O \rightarrow RO^{\cdot} \quad (27)$$

It is well established as such polymer alkoxy radicals ($RO^{\cdot}$) are the main species involved in the chain backbone scission of PP during oxidation through the well-known β-scission reaction (Figure 4).

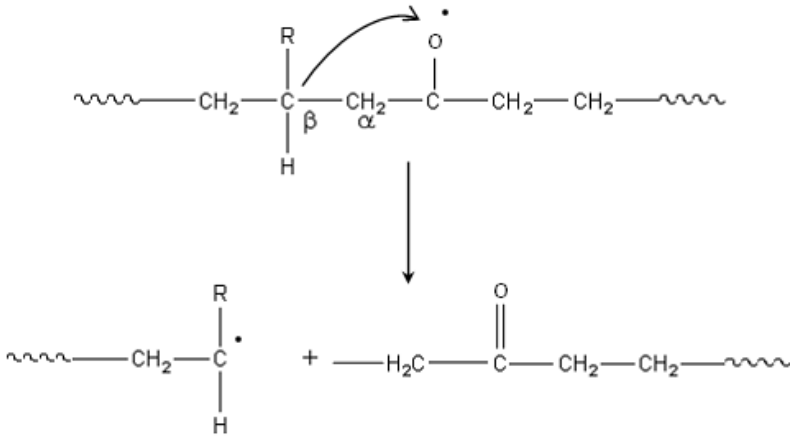

Figure 4. Schematic representation of a β-scission reaction on a polyolefin backbone.

Surface oxidation can also take place by additional routes; however, these tend to be less important than the aforementioned direct reaction with atomic oxygen. For example, the alkyl radicals ($R^{\cdot}$) can be attacked by molecular oxygen (O_2), yielding peroxy polymer radicals ($ROO^{\cdot}$), which in turn can abstract hydrogen from other polymer chains to produce polymer hydroxyperoxides (ROOH). All of these intermediates (alkoxy, peroxy, and hydroperoxy) can originate a large variety of oxidised species reacting with atomic oxygen, OH radicals, or even through cross-reaction with intramolecular polymer radicals [42]. Arising from these different reaction mechanisms, a wide range of new chemical groups can be inserted onto the polyolefin backbone. In particular, the formation of hydroxyl, carboxyl, and carbonyl groups is the most relevant concerning the increase in the wettability ad adhesion properties.

Finally, it is worth stressing the heterogeneity of oxidation on the polyolefin surface. This has been attributed to the different physical domains in a typical semi-crystalline polymer such as PP. More specifically, it seems that the regions most susceptible to treatment are those amorphous rather than crystalline. This fact would justify the scarce homogeneity in the extent of the oxidation, which is the basis of the hysteresis phenomenon that can be observed during contact angle measurements on flame-treated PP films.

7. Flame treatment equipment

Although conceptually similar, flame treaters used in packaging industries for polyolefin surfaces show obvious differences depending on whether the sample to be treated has a two-dimensional or three-dimensional geometry. In both cases, three main components can be recognised. For 3D objects, the plant typically consists of (Figure 5a):

1) a conveyor belt, which allows a continuous loop of material, i.e., the polyolefin objects, which are normally mounted on heat-resistant holders;
2) a cleaning device, such as a stream of compressed air or a brush-like system. This is normally placed a few centimetres in front of the burners to assure the removal of all small particles (e.g., dust) that might negatively affect successful flame treatment; and
3) a burner, i.e., the basic part of the equipment that produces the oxidising flame.

A typical plant for the flame treatment of polyolefin flexible films (Figure 5b) is instead conceived as follows:

1) a burner, which should produce a suitable flame for treating the surface of the web;
2) a treater roll, which is normally water-cooled. This enables the rewinding of the treated film and prevents any unwanted damage due to overheating; and
3) a nip roll, which is usually rubber-coated. Its function is to exert a certain pressure on the film to ensure the necessary contact between the web and the cooled roll. This prevents the formation of bubbles and/or blisters, which might otherwise impede the right thermal exchange between the web and the treater roll.

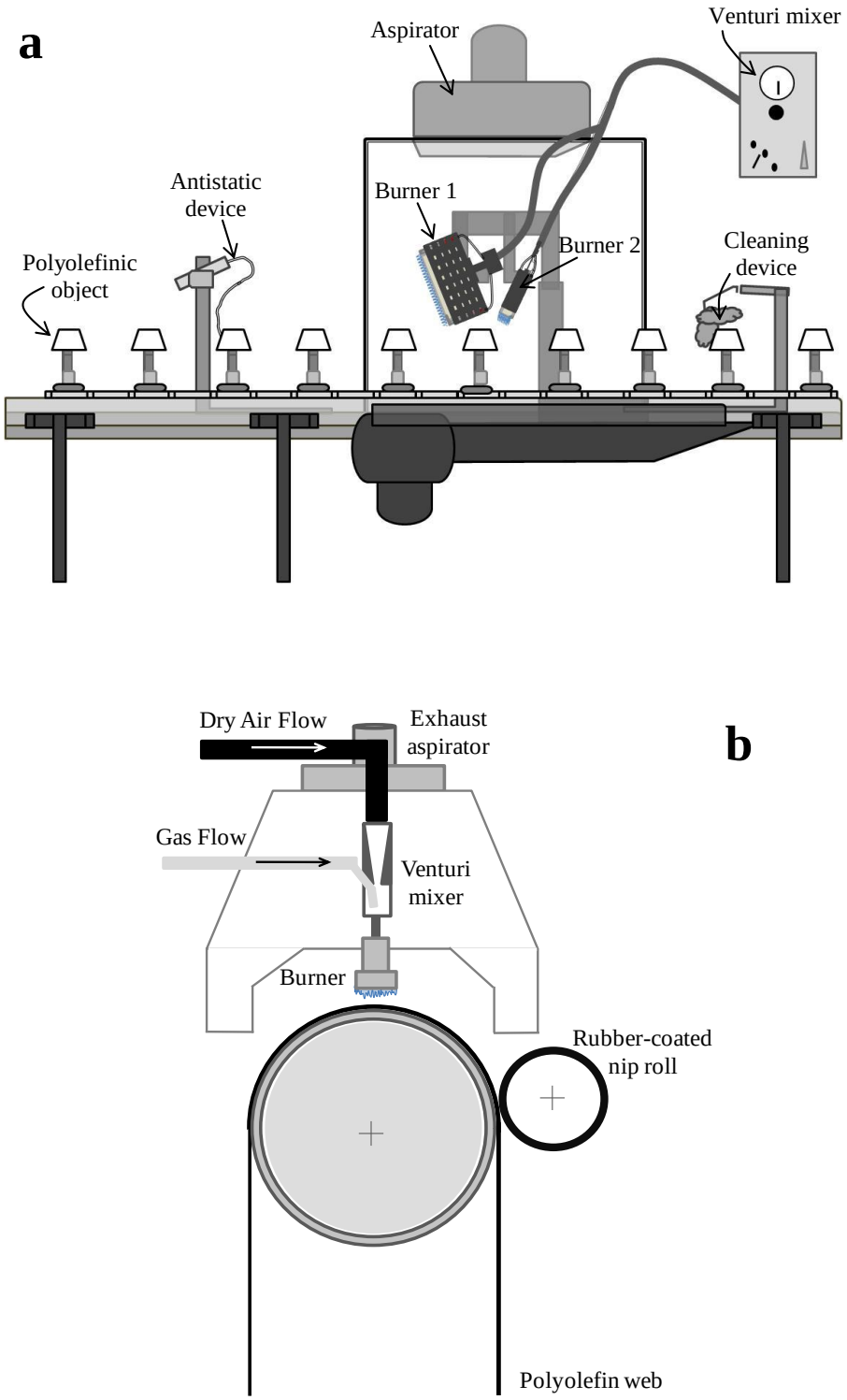

Figure 5. Schematic representation of a flame treatment station for polyolefin a) tridimensional objects and b) flexible films.

Certainly, the core of a typical flaming system is the burner. Nowadays, burners are complex parts affecting strongly the outcome of the whole process. Despite the wide range of burners available on the market, a common feature is the system that delivers the gas/air mixture to the burner nozzle (head) by exploiting the still valid principles developed by Venturi and Bunsen. Such a system, generally known as Venturi mixer, is located a few metres upstream of the burner. Burners fall into two main groups. Atmospheric burners are so called because part of the air used to generate the premixed fuel/air laminar flame is from the surrounding atmosphere, and is thereby at atmospheric pressure. This is because the gas entering the orifice at the base of the mixing tube is at low pressure (only a few inches of water column), providing only approximately 50% of the required air for the combustion. Consequently, the remainder is drawn from the environment around the nozzle, where the free air is usually conveyed by openings near the burner. An example of atmospheric air is the Bunsen burner. Contrary to atmospheric burners, power burners provide a powerful source of combustion air, making it possible to achieve higher energy output compared with atmospheric burners.

In an attempt to fulfil market requirements, different burners have been designed and developed over time, and a large variety of configurations are currently available. Gun-type nozzles were especially developed for the flame treatment of three-dimensional objects, where part of the gas/air mixture is deviated into small holes at a speed that is gradually reduced until continuous ignition is provided to the main gas/air flux coming out of the central orifice. This makes it possible to increase the velocity of the laminar flame out of the head of the burner, thereby achieving the targeted heat output. The burners used for flaming flexible films, e.g., polyolefins for the packaging industry, are based on a similar principle. In this case, the need to spread the flame on a wider front (i.e., equal to the width of the roll) led to developing pipe-like nozzles with a long array of drilled holes emitting the flame. On each side of this main row of drilled holes are smaller orifices, above which deflectors control the speed of the flame. So-called ribbon burners represent the last generation of burners available on the market. They consist of a regular shaped slot mounted with a

dimpled geometry ribbon stack. Such a design can reduce the speed of part of the gas/air mixture without needing devices such as deflectors or ignition rails. To date, the ribbon burner is the most widely adopted solution at an industrial level because it can attain customised flame patterns by adjusting the width of the slot and configuring the ribbons [44].

8. Flame treatment variables

8.1. Process variables

8.1.1. Gas/air ratio

The molar ratio of the fuel to the oxidiser is probably the most important parameter within the flame treatment process. For this reason, particular care must be paid to setting it adequately before the flame treatment is started. For each gas there exists a specific and well-defined amount of oxidiser at which the fuel is completely burnt. This precise ratio is known as the stoichiometric ratio, which relies on the chemical structure of the gas. For example, the stoichiometric ratio methane/air by mass is equal to 1:17.2, whereas for a propane/air flame it is 1:15.5, i.e., 15.5 kg of air is needed for the complete combustion of 1 kg of propane. However, in practical applications it is unlikely that the stoichiometric ratio can be verified. Most probably, the flame obtained will be below or above this value. Therefore, the concept of the equivalence ratio (ϕ), defined as the actual mass gas/air ratio used during treatment divided the stoichiometric fuel-to-oxidiser ratio [45], is widely accepted:

$$\phi = \frac{m_{fuel}/m_{oxidizer}}{(m_{fuel}/m_{oxidizer})_{stoichiometric}} \quad (28)$$

where m is the mass. The most common parameter is the reciprocal of the equivalence ratio, which is called the lambda factor and is expressed by the formula:

$$\lambda = \phi^{-1} \quad (29)$$

As a consequence, fuel-lean (oxidising) flames will have $\phi < 1$ and fuel-rich flames $\phi > 1$ (vice versa as far as the λ factor is concerned). Unambiguously, both λ and ϕ will be equal to the unit at

564 the stoichiometric ratio. It is worth pointing out that, for a given combustion system, the maximum
565 yield (expressed in terms of flame temperature) is achieved at the stoichiometric ratio, where
566 neither excess fuel nor excess oxidiser can be verified. Conversely, as ϕ veers from the
567 stoichiometric value (below and above), the flame temperature drops correspondingly (Figure 6).

568

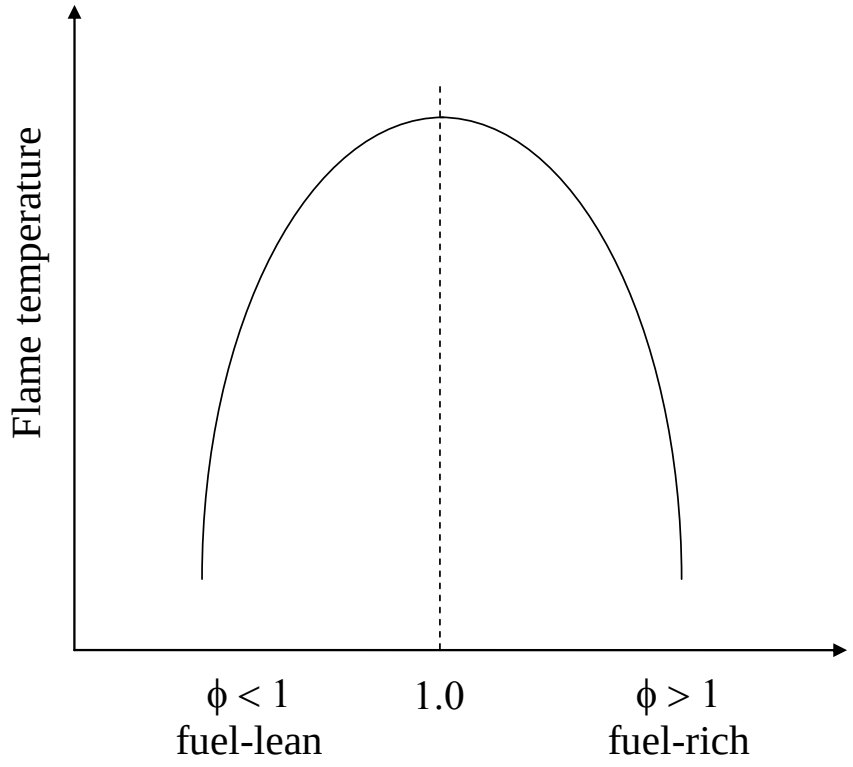

569

570 **Figure 6.** Flame temperature trend as a function of the equivalence ratio (ϕ).

571

572 This is because although excess fuel (or oxidiser flame) could never participate chemically in
573 the combustion reaction, it does affect the system from a physical point of view since, depending on
574 its specific heat value, such an excess tends to draw heat from the combustion system, thereby
575 causing the aforementioned decrease in yield. In practice, the most widely adopted configuration
576 foresees a fuel/air ratio slightly shifted to an oxidising flame composition (i.e., fuel-lean), because,
577 as mentioned previously, the web surface activation strictly depends on both flame temperature and
578 oxygen radical concentration. Thus, the best working condition can often be a compromise between

high flame temperature and oxygen radical content in the flame. It has been proven by many authors that oxidising flames ($0.75 < \phi < 1$) lead to the best surface activation of polyolefin substrates [46–49]. More recently, a detailed report by Strobel and co-workers [13] suggested the best performing equivalence ratio was 0.93 for all combinations of flame-to-film distance, flame power, and film speed using a methane/air mixture. At this optimum value, a maximum surface energy of approximately 62 mJ m^{-2} (according to the ASTM wetting test standard method [50]) was achieved. Accordingly, the highest ESCA O/C atomic ratio of flame-treated PP was recorded for equivalence ratio values ranging between 0.92 and 0.94, thereby following the same trend as the wettability measures. The authors concluded that such a high level of oxidation is the main reason for the increased wettability of the flame-treated PP surface.

8.1.2. Mixture flow

Based on the previous discussion, it is necessary to expose the polyolefin surface to a certain amount of thermal energy (heat) to achieve the desired activation of the web surface. Defining this quantity is not an easy task because the thermal energy required during the flaming process strongly relies on other parameters. Among them, it is worth mentioning flame power (i.e., the product of the volume of fuel burned per unit time and the heat content of the fuel, expressed in W), the exposure time of the film to the flame, the configuration of the burner, and the gap between the flame and film surface. However, a practical way to control the energy supplied to the web is to adjust the mixture flow (m^3 h^{-1}). Increasing the mixture flow leads to a corresponding increase in the treatment efficacy to a certain level (Figure 7, Q_1). Any mixture flow setting beyond this boundary value (Figure 7, Q_2) is profitless and causes unnecessary energy waste and thermal stress on the plastic film. Based on these principles, it has been possible to set down the relationship between mixture flow and flame treatment efficacy in terms of the surface energy of the treated surface.

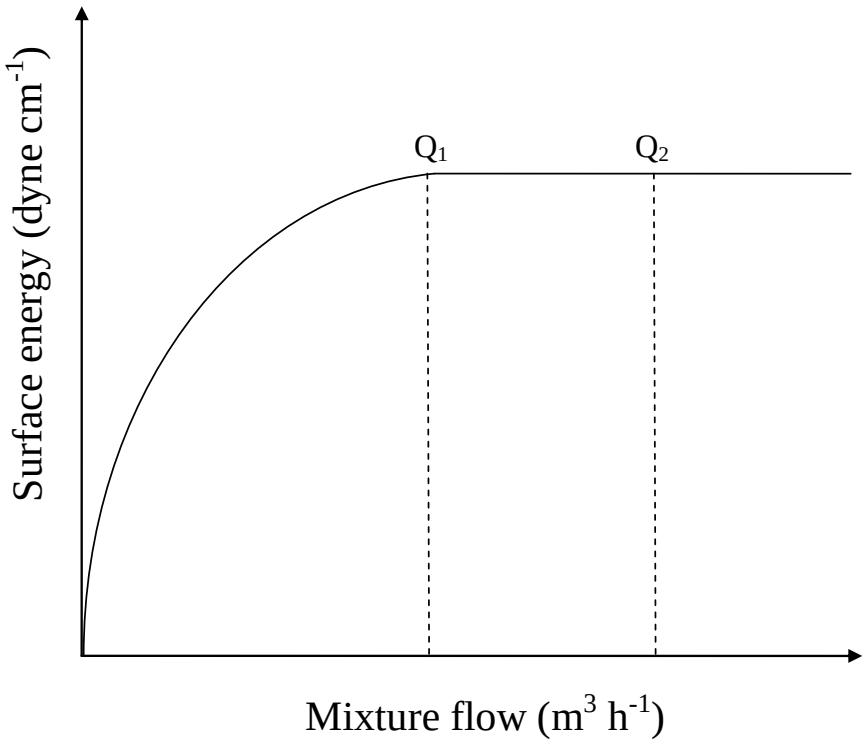

602

603 **Figure 7.** Surface energy evolution as a function of the gas/air mixture flow.

604

605 In Figure 8, the results obtained by our team for bi-oriented polypropylene (BOPP) at low and
606 high line speeds are reported (per unit of burner width). Such types of plots are useful tools for
607 pinpointing the best conditions for each specific application.

608 *8.1.3. Flame/surface gap*

609 It is widely recognised that the gap between the flame and web surface (i.e., the distance
610 between the tips of the luminous flame cones and polyolefin surface) is a key factor in determining
611 the extent of activation accomplished by the treatment. As a general trend, it has been observed that
612 when the film passes through the flame, a rapid depletion in the wettability of the treated surface
613 occurs. As the distance between the cone of the flame and film surface increases, surface activation
614 decreases, although a beneficial effect arising from the treatment is still appreciable up to
615 approximately 20 mm.

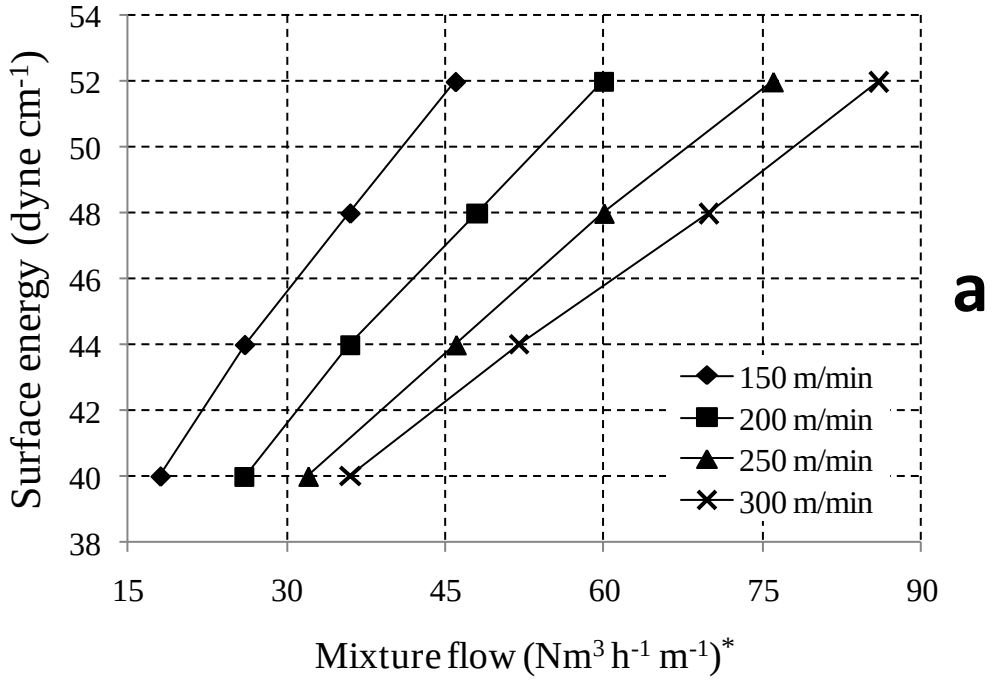

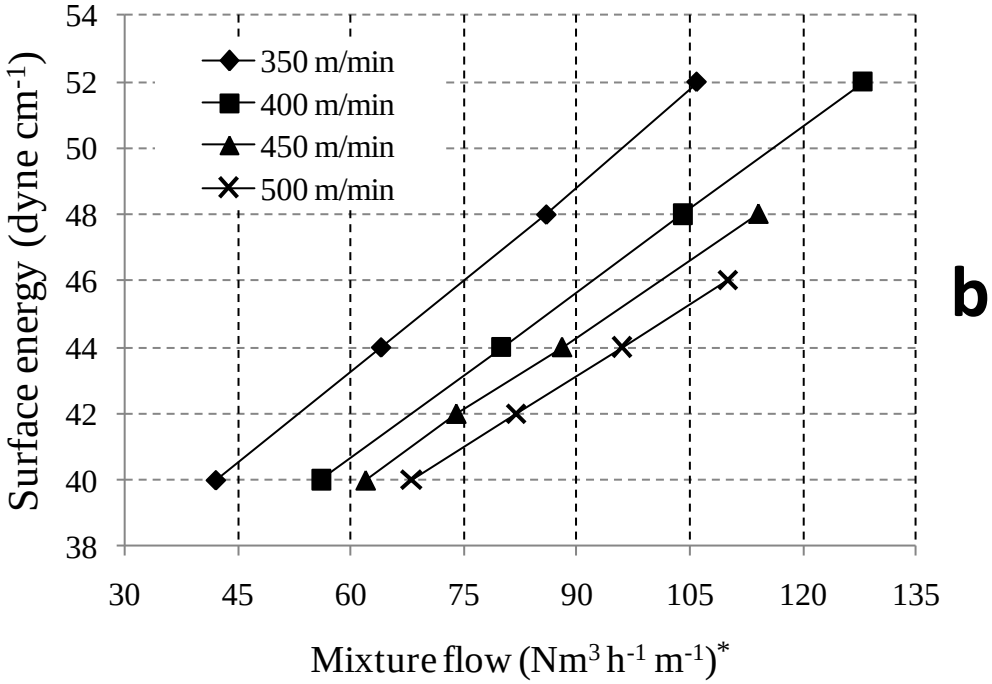

Figure 8. Influence of the mixture flow on the surface energy of treated BOPP at low (a) and high (b) speeds. *Normal cubic metres per hour, equal to one cubic metre under "normal" conditions, defined as 0°C and 1 atmosphere (101.3 kPa).

623 Many researchers have carried out empirical tests to set the optimum distance between the
624 flame and film surface. Ayers and Shofner suggested that the optimum distance was 0–6 mm above
625 the luminous flame front [51]. Sheng and co-workers pointed out that the most effective flame
626 treatment on the activation of PP webs is achieved 5–10 mm film-to-flame distance [52]. Other
627 authors concluded that to achieve the best wettability and oxidation of polyolefin surfaces, the
628 distance between the tips of the flame cones and web surface should be less than 10 mm [46]. The
629 conclusions by Strobel and co-workers confirm further the tendency to position the film slightly
630 beyond the luminous cone [13]. The authors fixed the right film-to-flame gap at 2 mm for a PP film
631 treated with a methane/air mixture at a 0.93 equivalence ratio. These findings are consistent with
632 the flame profile theory discussed above. Indeed, to maximise the benefit from the treatment, the
633 flame should work in tandem with its luminous zone, which is the richest in active oxidising species
634 (OH radicals and O atoms) and the one at the highest temperature within the whole combustion
635 system. Conversely, when the film-to-flame distance is set below 1.5–2.0 mm, the part of the flame
636 involved is the 'dark zone'. Here, the contribution by the flame temperature is negligible and the
637 reactive oxidising species are almost absent. Rather, this zone has plenty of hydrogen radicals,
638 which tend to recombine with oxygen radicals and thereby act as a limiting factor in the oxidation
639 mechanism of the film surface. Analogously, placing the film surface further than 1.5–2.0 mm from
640 the tips of the luminous flame cones would mean the flame treatment would be less effective than in
641 the luminous zone. However, since both the flame temperature and oxygen radical concentration are
642 higher in this region (post-combustion) than in the dark zone, some positive effect because of the
643 flame is still detectable on the treated film surface. This fact explains the typical aspect of the curve
644 obtained by plotting the surface energy values as a function of the film-to-flame distance. As shown
645 in Figure 9, this curve is asymmetric with respect to the maximum surface energy value found at a
646 film-to-flame distance of approximately 2 mm, indicating that the positive effect of flame treatment
647 is still somehow evident in the post-combustion zone, whereas it quickly drops to zero in the dark
648 region.

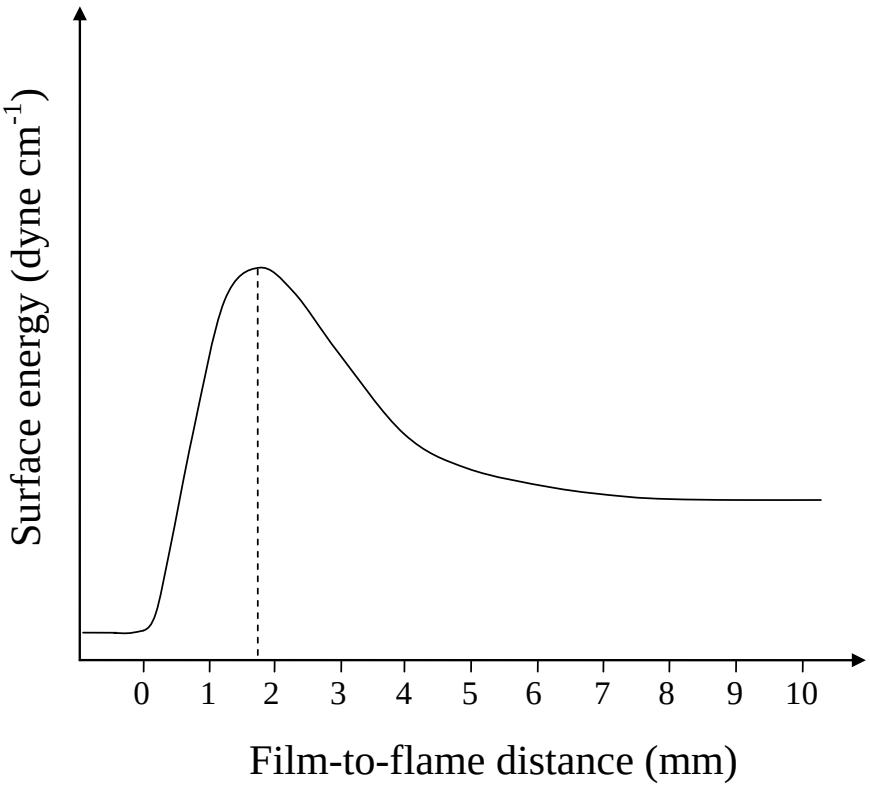

649

650 **Figure 9.** General trend of the surface energy values of flame-treated polyolefin films as a function
651 of the film-to-flame gap.

652

653 *8.1.4. Temperature and relative humidity external conditions*

654 The temperature (T) and relative humidity (RH) of the surroundings are often underestimated
655 parameters during flame treatment, but these can greatly affect the final outcome of the process
656 because increases in either can cause a shift in the gas/air mixture towards a fuel-rich composition,
657 thereby provoking a dramatic change in the properties of the treated surface of the polyolefin film.
658 The influence of both temperature and relative humidity is schematically displayed in Figure 10.
659 Here, it is possible to observe that the value of λ diverges from its initial setting (~1.04) owing to an
660 increase in temperature and relative humidity. This diagram was obtained from natural gas (relative
661 density = 0.59) under the hypothesis that the mixture is in the stoichiometric condition at T = 20°C
662 and RH = 0%. Based on these considerations, a systematic check of the gas/air mixture is deemed
663 necessary to keep it constant, regardless of the influence of external conditions. For this purpose, a

664 wide variety of portable and online devices enabling the measurement of any variation in λ due to
665 changes in room conditions, are available on the market.

666

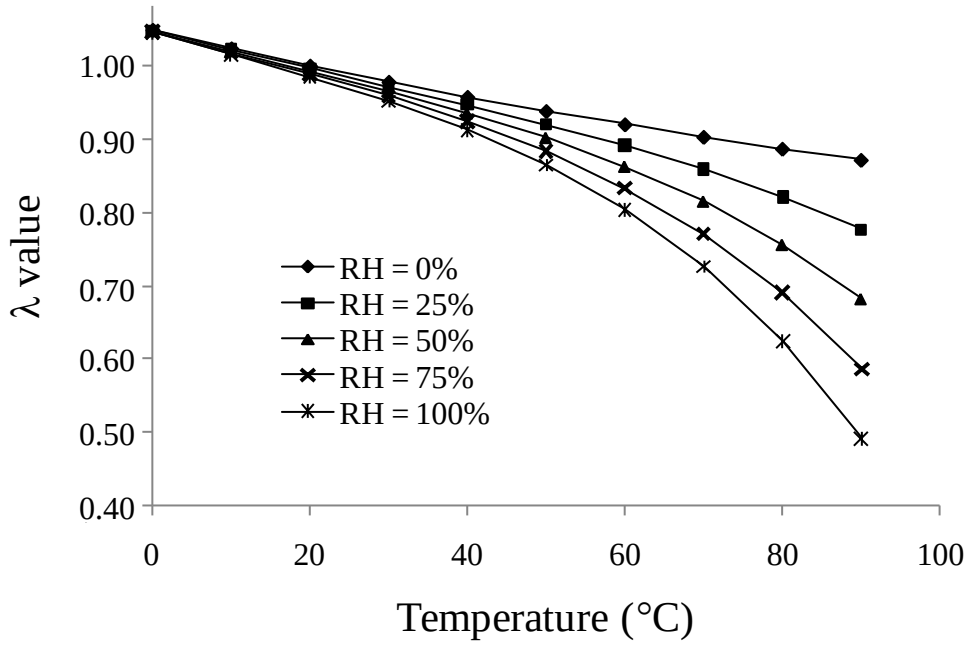

667

668 **Figure 10.** Influence of room conditions (temperature and relative humidity) on the λ value of a
669 stoichiometric (T = 20°C; RH = 0%) natural gas (d_r = 0.59)/air mixture.

670

671 *8.1.5. Number of sequential treatments*

672 A final aspect that should be carefully taken into consideration is the number of treatments to
673 which the film surface has been submitted. Although it strongly depends on other aspects (i.e.,
674 flame temperature, flame flow, flame-to-film distance), some general considerations can help carry
675 out the appropriate treatment. Contrary to what common sense might suggest, increasing the
676 number of treatments in the same sample does not imply a proportional increase in the surface
677 properties of the polyolefin surface. Indeed, in particular when high temperatures are reached,
678 overtreatment lead to surface reorganisation in the modified polymer surface. Two different
679 phenomena have been highlighted in this respect [8]. On one hand, as a result of overtreatment, the
680 oxygen-containing functional groups inserted in the first step of treatment can disappear from the

surface. On the other hand, high temperatures can trigger the migration of the additives normally included in polyolefin compounds, such as heat stabilisers, release agents, antistatics, and UV stabilisers. In both cases, the final result is the same: the wettability and adhesion properties of the plastic surface are irremediably compromised and the successful deposition of paints, inks, or whatever coating will be hindered. To prevent these detrimental effects, when planning more than one treatment on the same sample it is very important to avoid excessively short time intervals between two sequential flames to allow the heat generated by the flame to dissipate properly.

8.2. Sample variables

8.2.1. Surface contaminations

Although often underestimated, the potential presence of contaminants on the plastic surface is an important aspect to face, since it directly influences the efficacy of flame treatment. Probably because of the high potency associated with a flame, a common misconception is that to activate a polyolefinic surface, flame treating it using a proper fuel/air mixture is the only prerequisite. Instead, the activation step is a necessary but insufficient condition to assure durable adhesion at the polyolefin substrate/coating interface. Contaminations of samples can originate from different causes, for example, the manufacturing processes and storage conditions of the polyolefinic substrates. Even though they are not always easy to detect, typical residuals can be found on the surface of finished objects, such as spots of the releasing agents commonly used in the injection moulding process (e.g., silicones), additives migrated from the bulk (plasticisers, antioxidants), or, more simply, dust. Irrespective of the origin, the final effect will be the inhibition (more or less deeply depending on the extent of the contamination) of the surface activation promoted by the flame. This is because of the 'shield effect', whereby the contaminant screens regions of the polymer susceptible to chemical modifications mediated by the treatment. Therefore, following the flaming, a lower amount of chemical modifications will be found per unit of the treated area. As an ultimate consequence, the deposition of whatever coating will be dramatically affected in those

zones of the plastic substrate lacking adequate wettability. To counteract these considerations, the proper cleaning step of the polyolefin surface should be always planned, especially for long-term adhesion durability. This can be achieved in different ways. Among them, blow-off dust devices (generally in the form of brush), nitrogen gas steam, and solvent degreasing are the most widely used strategies. The final choice greatly depends on the shape of the samples and specific manufacturing constraints.

8.2.2. Topography of the surface

It is well established that the wettability of a polymer surface is strongly affected by its topography. In this respect, two major theories can explain the effect of the roughness of the surface on its wettability behaviour: the Wenzel theory [53,54] and the Cassie-Baxter theory [55], which differ from Young's theory that applies only to perfectly smooth surfaces [56]. Although the surface morphology affects the wettability properties, the extent of the flame treatment also seems to be influenced by this parameter. Our preliminary results corroborate this hypothesis. Injection-moulded PP (nucleated heterophasic copolymer, Basell Polyolefins srl, Ferrara, Italy) square plates (40 mm width, 3 mm thick) at different topographies (highly rough – H, medium-sized roughness – M, and perfectly smooth – S) were analysed by atomic force microscopy (AFM) before (Figure 11) and after (Figure 12) flame treatment. The three untreated samples exhibited a noticeable difference in topography. The smooth PP plates had a RMS roughness of approximately 390 nm, whereas the mean roughness of the M and H samples was in the order of 550 nm and 1.34 μm, respectively. However, apparently out of line with the aforementioned theories, both water contact angle and surface energy values of the three untreated samples (103.5 ± 2.51° and 28.74 ± 0.64 dyne cm^{-1} for S samples, 103.1 ± 2.21° and 29.08 ± 0.72 for M samples, and102.3 ± 2.66° and 29.37 ± 0.88 dyne cm^{-1} for H samples) were quite similar, presumably because the differences in roughness between samples were too narrow to justify statistically significant distinctions. When subjected to the same flame treatment (propane/air mixture with λ = 1.028; flame contact time = 0.05 s; film-to-flame

distance = 2.0 mm), all samples revealed a distinct reduction of RMS roughness, which amounted to 270 nm, 340 nm, and 490 nm for samples S, M, and H, respectively.

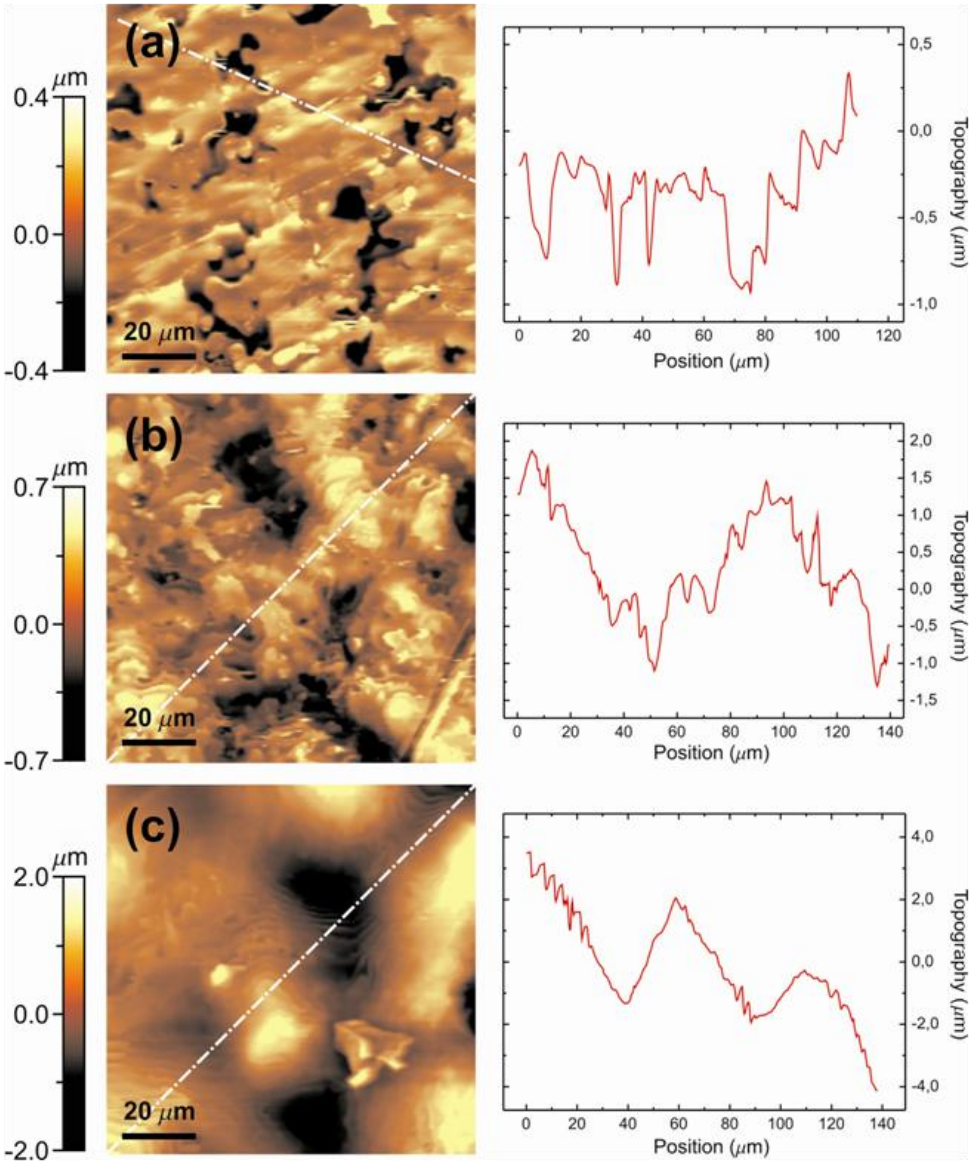

Figure 11. Left column: 100 x 100 μm^2 AFM height images of: a) perfectly smooth – S; b) medium-sized roughness – M, and c) highly rough – H polypropylene untreated (non-flamed) samples. Right column: profile along the dash-dotted line from the corresponding height image.

Noticeably, a clear dependence of the surface response to a given flame treatment on the average roughness was found by optical contact angle and surface energy measurements, which amounted to 72.98 ± 4.8° and 39.19 ± 0.67 dyne cm^{-1} for S samples, 50.23 ± 3.6° and 44.53 ± 0.58

742 dyne cm^{-1} for M samples, and 40.43 ± 2.24° and 48.89 ± 0.75 dyne cm^{-1} for H samples. A clear
743 trend is therefore demonstrated, with the roughest surface being also the most sensible to flame
744 treatment (i.e. leading to the largest variations in its own wettability properties).
745

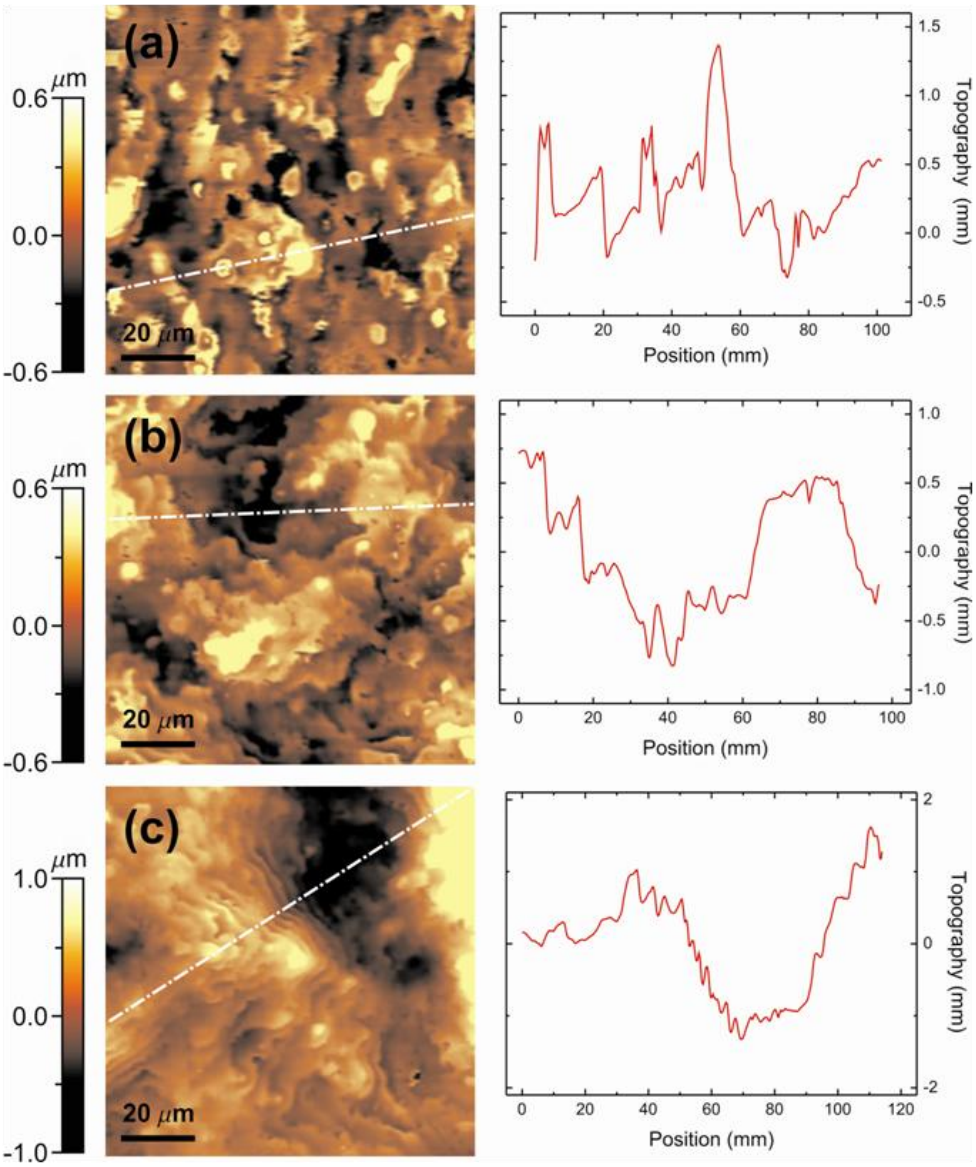

746

747 **Figure 12.** Left column: 100 x 100 μm^2 AFM height images of: a) perfectly smooth – S; b)
748 medium-sized roughness – M, and c) highly rough – H polypropylene flame-treated samples. Right
749 column: profile along the dash-dotted line from the corresponding height image.
750

751

Although the total effective exposed surface area for the untreated rough samples is not considerably larger than that of smooth samples (less than 10% difference), a tentative explanation for this trend should likely consider that the amount of polyolefinic substrate exposed to the flame (per unit area) increased proportionally to the roughness of the sample. According to this hypothesis, the roughest samples would be oxidised to a larger extent than the smoothest ones.

It is also worth noting that AFM images of treated samples clearly revealed, within our spatial resolution, that other relevant structural changes occurred at the surface of S samples (Figure 12a), with the appearance of small, evenly distributed agglomerates on the treated surface, with dimensions in the order of 0.5 – 1.0 μm in height and few microns in width (Figure 13). On the contrary, height images captured from samples M and S did not show any apparent evolution from this point of view after the treatment (Figure 12b and 12c, respectively). This observation suggests a further likely scenario. Owing to the flame treatment, it might be plausible that the S samples underwent a reorganisation at the surface level, as already postulated in an earlier paper [8]. Whether such modifications rely on the migration of additives from the bulk to the surface of the polymer because of the high temperature or on the disappearing of oxygen-containing groups from the surface is still unknown. X-ray photoelectron spectroscopy, confocal Raman microscopy, and FTIR-ATR spectroscopy analyses currently carried out within our group should provide our ongoing research with further elucidations.

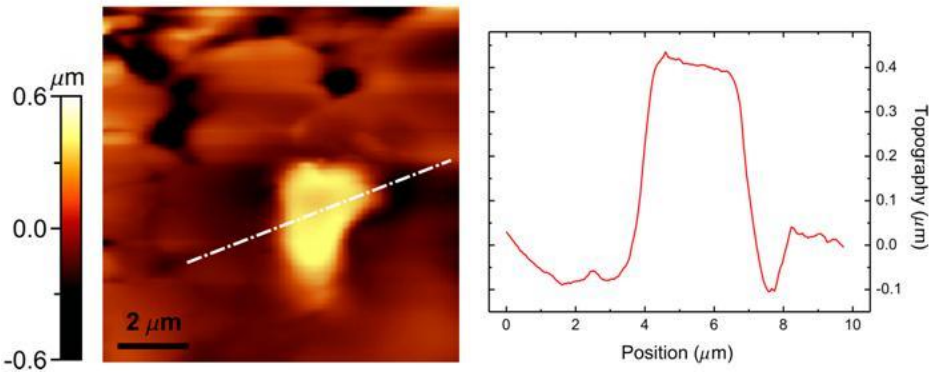

Figure 13. Magnified topography of an aggregate from the height image in Figure 12a and corresponding section along the dash-dotted line.

9. Concluding remarks

Flame treatment is a powerful technique for enhancing the surface attributes of plastic materials, especially those with a marked inherent hydrophobicity such as polyolefins. However, its potential has not been completely capitalised so far for two main reasons: 1) the lack of familiarity with the principles governing the combustion phenomena; and 2) the high number of parameters affecting the overall flame treatment process, which make the initial tweak of the flame equipment time consuming and frustrating, especially compared with alternative techniques such as the corona discharge, which is nowadays widely used in specific applications such as the treatment of polyolefin films intended for packaging applications.

Although it has not been possible to address all topics related to the flame phenomenon, this review has attempted to provide the basic tools to rationally exploit flame treatment at both an industrial and academic level. Our discussion was based on some major guiding principles. Firstly, without knowing the underlying fundamentals of flame chemistry it is difficult to manage the flame phenomena in any application. Secondly, knowing the most important controlling factors of the overall process and being aware of how these parameters can affect the final outcome is of utmost importance to gain the maximum benefit from the treatment. Thirdly, it is essential to understand how to control the process variables to keep the flame treatment setting as standardised as possible, because even minimal changes can cause huge deviations in the expected results, i.e., the low surface activation of treated surfaces. Therefore, controlling accurately all parameters throughout the process represents a major task that cannot be procrastinated longer in any industrial application envisaging using flame to activate polymer surfaces. It is important to stress that although generally valid, the concepts outlined in this review do not apply in any circumstance; hence, some aspects need to be faced separately depending on the specific application. For example, the influence of the substrate has to be regarded carefully, since different polyolefin types are affected in different ways by modification treatment. Therefore, tailored operative conditions have to be pinpointed accordingly.

A systematic approach to using flame as a surface-activation technique is not only necessary for obtaining reproducible results but would decisively encourage the future development of new structures. This notion is supported by strong recent research attention on the potential use of biomacromolecules in many applications, such as within the packaging industry, motivated by the growing needs for more sustainable solutions. To address this issue, many researchers have suggested a way of generating new optimised structures, in which the use of plastic resins should be less of a driving force to lighter configurations without jeopardising the overall performance of the package. This can be attained by replacing multi-layered architectures with high performance thin coatings. In addition, recent advancements in the coatings field have provided the opportunity of fabricating composite structures by laying plastic substrates with water-based bio-coatings (i.e., obtained from molecules of natural origin). Among other benefits, this would allow cleaner processes, since the use of organic solvents normally used for synthetic coatings is avoided. However, the deposition of totally waterborne coatings onto polyolefin surfaces is a tough target because of the higher surface tension of water-based coatings compared with current formulations. With this scenario in mind, a remarkable contribution could arise from flame treatment becoming a leading technique for the surface activation of inherently hydrophobic polymers. This can be accomplished not only by appropriately using this technique but also finding out new setting conditions and technical advancements that would achieve very high surface energy values on treated surfaces. This would make it possible to use totally water-based solutions, paving the way for new structures that have not yet been obtained, e.g., polyolefins/bio-based coating pairs. Certainly, worldwide research activity can greatly help this challenge over future years.

References

1) Awaja F, Gilbert M, Kelly G, Fox B, Pigram PJ. Progress in Polymer Science 2009; 34: 948–968.
2) Poisson C, Hervais V, Lacrampe MF, Krawczak P. Journal of Applied Polymer Science 2006; 101: 118–127.
3) Tomasetti E, Daoust D, Legras R, Bertrand P, Rouxhet PG. Journal of Adhesion Science and Technology 2001; 15: 1589–1600.
4) Kumar CR, George KE, Thomas S. Journal of Applied Polymer Science 1996; 61: 2383–2396.
5) Lee KT, Goddard JM, Hotchkiss JH. Packaging Technoly and Science 2009; 22: 139–150.
6) Molitor P, Barron V, Young T. International Journal of Adhesion and Adhesives 2001; 21: 129–136.
7) Wingfield JRJ. International Journal of Adhesion and Adhesives 1993; 13: 151–156.
8) Pijpers AP, Meier RJ. Journal of Electron Spectroscopy and Related Phenomena 2001; 121: 299–313.
9) Baldan A. Journal of Materials Science 2004; 39: 1–49.
10) Strobel M, Jones V, Lyons CS, Ulsh M, Kushner MJ, Dorai R, Branch MC. Plasmas and Polymers 2003; 8: 61–95.
11) Tracton AA. Coatings technology handbook. CRC Press: Boca Ranton, FL, USA, 2006.
12) Maltese P, Olivieri P, Protospataro F. Il polipropilene: una storia italiana. Tyrus: Terni, Italy, 2003.
13) Strobel M, Branch M, Ulsh M, Kapaun RS, Kirk S, Lyons CS. Journal of Adhesion Science and Technology 1996; 10: 515–539.
14) Faraday M. The chemical history of a candle. Dover Publications: Mineola, NY, USA, 2002.
15) Glassman I, Yetter R. Combustion, 4th edition. Academic Press: San Diego, CA, USA, 2008.
16) Westbrook CK, Dryer FL. Progress in Energy and Combustion Science 1984; 10: 1–57.
17) Vandooren J, Branch MC, Van Tiggelen PJ. Combustion and Flame 1992; 90: 247–258.

851 18) Galloway JN, Dentener FJ, Capone DG, Boyer EW, Howarth RW, Seitzinger SP, Asner GP,
852 Cleveland CC, Green PA, Holland EA, Karl DM, Michaels AF, Porter JH, Townsend AR,
853 Vöosmarty CJ. Biogeochemistry 2004; 70: 153–226.
854 19) Richter GN, Wiese HC, Sage BH. Combustion and Flame 1962; 6: 1–8.
855 20) Glassman I. Combustion. Academic Press: San Diego, CA, USA, 1996.
856 21) Tanford C, Pease RN. Journal of Chemical Physics 1947; 15: 433–439, 861–865.
857 22) Zeldovich YB, Frank-Kamenetskii DA. Zhurnal Fizicheskoi Khimii 1938; 12: 100–105.
858 23) Semenov NN. Nature 1943; 151: 185–187.
859 24) Semenov NN. Chain reactions. Goskhimtekhizdat: Leningrad, 1934.
860 25) Mallard E, Le Chatelier H. Annales des Mines 1883; 8: 274–568.
861 26) Clingman WH, Brokaw RS, Pease R. Fourth Symposium (International) on Combustion (The
862 Combustion Institute, Pittsburgh, Pennsylvania) 1953; 310–313.
863 27) Rahim F, Elia M, Ulinski M, Metghalchi M. International Journal of Engine Research 2002; 3:
864 81–92.
865 28) Elia M, Ulinski M, Metghalchi M. Journal of Engineering for Gas Turbines and Power 2001;
866 123: 190–196.
867 29) Yu CL, Wang C, Frenklach M. Journal of Physical Chemistry 1995; 99: 14377–14387.
868 30) Westbrook CK, Dryer FL. Combustion and Flame 1980; 37: 171–192.
869 31) Westbrook CK, Dryer FL. Eighteenth Symposium (International) on Combustion (The
870 Combustion Institute, Pittsburgh, Pennsylvania) 1981; 749–767.
871 32) Westbrook CK. Combustion and Flame 1982; 46: 191–210.
872 33) Tieszen SR, Stamps DW, Westbrook CK, Pitz WJ. Combustion and Flame 1991; 84: 376–390
873 34) Papirer E, Wu DY, Schultz J. Journal of Adhesion Science and Technology 1993; 7: 343–362.
874 35) Garbassi F, Occhiello E, Polato F, Brown A. Journal of Materials Science 1987; 22: 1450–
875 1456.
876 36) Briggs D, Brewis DM, Konieczko MB. Journal of Materials Science 1979; 14: 1344–1348.

877 37) Garbassi F, Occhiello E, Polato F, Brown A. Journal of Materials Science 1987; 22: 1450–
878 1456.
879 38) Dillard JG, Cromer TF, Burtoff CE, Cosentino AJ, Cline RL, MacIver GM. Journal of
880 Adhesion 1988; 26: 181–198.
881 39) Sheng E, Sutherland I, Brewis DM, Heath RJ. Applied Surface Science 1994; 78: 249–254.
882 40) Strobel M, Walzak MJ, Hill JM, Lin A, Karbashewski E, Lyons CS. Journal of Adhesion
883 Science and Technology 1995; 9: 365–383.
884 41) Kee RJ, Grcar JF, Smooke MD, Miller JA. FORTRAN Program for modeling steady one-
885 dimensional premixed flames. Report SAND85-8240. Sandia National Laboratories, Livermore,
886 CA (1989).
887 42) Clouet F, Shi MK. Journal of Applied Polymer Science 1992; 46: 1955–1966.
888 43) Hansen RH, Pascale JV, De Benedictis T, Rentzepis PM. Journal of Polymer Science Part A
889 1965; 3: 2205–2214.
890 44) Tracton AA. Coatings Technology Handbook. CRC Press: Boca Ranton, FL, USA, 2006.
891 45) Pitts WM. Progress in Energy and Combustion Science 1995; 21: 197–237.
892 46) Dillard JG, Cromer TF, Burtoff CE, Cosentino AJ, Cline RL, Maciver GM. Journal of
893 Adhesion 1988; 26: 181–198.
894 47) Sheng E, Sutherland I, Brewis DM, Heath RJ. Applied Surface Science 1994; 78: 249–254.
895 48) Sutherland I, Brewis DM, Health RJ, Sheng E. Surface and Interface Analysis 1994; 17: 507–
896 510.
897 49) Brewis DM. Journal of Adhesion 1992; 37: 97–107.
898 50) ASTM. Standard Test Method for Wetting Tension of Polyethylene and Polypropylene Films.
899 Designation D 2578-84. American Society for Testing and Materials.
900 51) Ayers RL, Shofner DL. SPE Journal 1972; 28: 51–55.
901 52) Sheng E, Sutherland I, Brewis DM, Heath RJ, Bradley RH. Journal of Materials Chemistry
902 1994; 4: 487–490.

903 53) Wenzel RN. Industrial & Engineering Chemistry 1936; 28: 988–994.
904 54) Rosario R, Gust D, Garcia AA, Hayes M, Taraci JL, Clement T, Dailey JW, Picraux ST.
905 Journal of Polymer Science - Part B: Polymer Physics 2004; 108: 12640–12642.
906 55) Wu X, Zheng L, Wu D. Langmuir 2005; 21: 2665–2667.
907 56) Morra M, Occhiello E, Garbassi F. Advances in Colloid and Interface Science 1990; 32: 79–
908 116.